HHS Public Access

Author manuscript

Am J Med Genet A. Author manuscript; available in PMC 2017 November 05.

Published in final edited form as:

Am J Med Genet A. 2015 June ; 167(6): 1374–1380. doi:10.1002/ajmg.a.37047.

MED23-associated Intellectual Disability in a Non-consanguineous Family

Aditi Trehan[1,2], **Jacqueline M. Brady**[1,2], **Valerie Maduro**[1,2], **William Bone**[1,2], **Yan Huang**[1,2], **Gretchen A. Golas**[1,2], **Megan Kane**[2], **Paul R. Lee**[3], **Audrey Thurm**[4], **Andrea L. Gropman**[1,5], **Scott M. Paul**[6], **Gilbert Vezina**[5], **Thomas C. Markello**[2], **William A. Gahl**[1,2], **Cornelius F. Boerkoel**[2], and **Cynthia J. Tifft**[1,2]

[1]Office of the Clinical Director, NHGRI/NIH, Bethesda, Maryland, USA

[2]NIH Undiagnosed Diseases Program, NIH Office of Rare Diseases Research and NHGRI, Bethesda, Maryland, USA

[3]National Institute of Neurological Disorder and Stroke, NIH, Bethesda, Maryland, USA

[4]Pediatrics and Developmental Neuroscience, NIMH/NIH, Bethesda, Maryland, USA

[5]George Washington University School of Medicine and Health Sciences and Children's National Medical Center, Washington D.C., USA

[6]Rehabilitation Medicine Department, Clinical Center, NIH, Bethesda, Maryland, USA

Abstract

Intellectual disability (ID) is a heterogeneous condition arising from a variety of environmental and genetic factors. Among these causes are defects in transcriptional regulators. Herein, we report two brothers in a non-consanguineous family with novel compound heterozygous, disease-segregating mutations (NM_015979.3: [3656A>G];[4006C>T], NP_057063.2: [H1219R]; [R1336X]) in *MED23.* This gene encodes a subunit of the Mediator complex that modulates the expression of RNA polymerase II-dependent genes. These brothers, who had profound ID, spasticity, congenital heart disease, brain abnormalities, and atypical electroencephalography, represent the first case of *MED23*-associated ID in a non-consanguineous family. They also expand upon the clinical features previously reported for mutations in this gene.

Keywords

Intellectual Disability (ID); MED23; Mediator Complex; Whole Exome Sequencing (WES)

INTRODUCTION

Intellectual disability (ID) is a significant limitation in cognitive functioning and a lack of adaptive skills necessary for daily living [APA, 2013]. As a neurodevelopmental disorder with a substantial lifelong burden, ID adversely influences the affected individual, the family

Corresponding author: Cynthia J. Tifft, Bldg. 10 CRC3-2551 MSC 1205, 10 Center Dr., Bethesda, MD 20892-1205, 301-451-8485 (voice), 301-496-7157 (fax), cynthiat@mail.nih.gov.

and/or caretakers, and the educational system. The diagnosis of ID involves: 1) deficits in intellectual functioning (IQ less than 70); 2) limitations in adaptive skills, such as communication, social participation and independent living; and 3) onset of symptoms before 18 years of age [APA, 2013]. Depending on the level of impairment in conceptual, social and practical domains, ID can be classified as mild, moderate, severe, or profound. In addition, ID is categorized as syndromic or non-syndromic based on the presence or absence of co-morbid features [Kaufman, Ayub, and Vincent, 2010].

Recent reports have linked ID and other related neurological disorders to mutations in more than 450 different genes, many of which encode proteins essential for transcriptional regulation, such as components of the Mediator complex [Van Bokhoven, 2011]. This complex is a multi-subunit assembly that relays signals from upstream enhancer elements to downstream RNA polymerase II machinery. Mutations in subunits of the Mediator complex, including MED12, MED17, and MED25, have been associated with cognitive impairment, brain abnormalities and/or neuromuscular deficits [Risheg et al., 2007; Schwartz et al., 2007; Kaufman, Straussberg, et al., 2010; Leal, et al., 2009]. A large consanguineous Algerian family showed cosegregation of non-syndromic autosomal recessive ID with a homozygous mutation in *MED23*, the gene encoding a subunit within the tail region of the Mediator complex [Hashimoto et al., 2011]. This mutation disrupted the ability of MED23 to interact with enhancer-bound transcription factors, TCF4 and ELK1, resulting in the dysregulation of immediate early genes (*JUN* and *FOS*) necessary for brain development and neuroplasticity.

We present two male siblings with profound ID and novel disease-segregating mutations in *MED23*. These brothers, who are the first MED23-deficient patients reported from a non-consanguineous family, expand the phenotype associated with mutations in this gene to include profound ID, spasticity, congenital heart disease, brain abnormalities, and atypical electroencephalography (EEG).

MATERIALS AND METHODS

Patients

The propositi were admitted to the National Institutes of Health Clinical Center (NIH-CC) and enrolled in protocol 76-HG-0238, “Diagnosis and Treatment of Patients with Inborn Errors of Metabolism or Other Genetic Disorders,” approved by the National Human Genome Research Institute (NHGRI) Institutional Review Board (IRB). After parents gave informed consent, the children were investigated at two different time points, i.e., ages 8 and 11 years for patient 1 and ages 23 months and 5 years for patient 2.

Exome Analysis

Genomic DNA was extracted from peripheral whole blood of the two affected individuals, their unaffected parents, and two unaffected siblings using the Gentra Puregene Blood Kit (Qiagen, Valencia, CA). The DNA of all family members was subjected to an integrated set of genomic analyses including high-density single-nucleotide polymorphism (SNP) arrays and whole exome sequencing (WES). WES was performed on the nuclear family using the Illumina HiSeq2000 platform and the TrueSeq capture kit (Illumina, San Diego, CA).

Sample library preparation, sequencing and analysis were performed using the standard NIH Intramural Sequencing Center (NISC) pipeline [NISC Comparative Sequencing Program, 2014]. Sequence data was aligned to human reference genome (hg19) using Novoalign (Novocraft Technologies, Selangor, Malaysia). To test for copy number variants and to form segregation BED files for exome analysis, Omni Express 12 (hg18) SNP arrays were run on genomic DNA from all family members as described [Markello et al, 2012] and converted to hg19. Variants listed in the Variant Call Files (VCFs) were filtered based on rarity, Mendelian segregation, and predicted deleteriousness. Allele frequencies were required to be < 0.06 for the UDP patient cohort and < 0.02 for the Exome Sequencing Project v.0.0.20 African Ancestry population, Exome Sequencing Project v.0.0.20 European Ancestry population, and dbSNP build 137. Also, homozygous and *de novo* variants were required to occur in < 2 individuals in the UDP cohort (excluding the affected brothers). Variants needed to segregate with autosomal recessive, X-linked recessive, or *de novo* dominant modes of inheritance and be annotated as nonsynonymous, frame shift, premature stop, loss of start codon, loss of stop codon, near splice (within 20 base pairs of a canonical splice site), or splicing mutations. Variants that passed filtration were ranked using Exomiser 2.0 (http://www.sanger.ac.uk/resources/databases/exomiser/query/exomiser2); the shared Human Phenotype Ontology terms of the patients were used as the phenotype input for Exomiser. Using the Integrative Genome Viewer (https://www.broadinstitute.org/igv/home), we assessed the quality of alignment and genotype call of variants.

Sanger DNA sequencing was used to validate the variants identified. Using the primers listed in Supplementary Table 1, PCR amplification was performed using Qiagen HotStarTaq master mix (Qiagen, Valencia, CA). The following conditions were used for amplification: 1 cycle of 95°C for 5 minutes, followed by 39 cycles of 95°C for 30 seconds, 55°C for 30 seconds, 72°C for 30 seconds, and a final extension at 72°C for 5 minutes. Unincorporated primers and nucleotides were removed using ExoSAP-IT reagent (USB, Cleveland, OH, USA). Sanger sequencing of the PCR products was performed by Macrogen (Rockville, MD). The sequences were aligned and analyzed using Sequencher v.5.0.1 (Gene Codes, Ann Arbor, MI, USA). CLIA certification was performed by Sanger DNA sequencing (Gene Dx, Rockville, MD).

Gene Expression Analysis

Skin fibroblasts were obtained from both patients under NHGRI IRB-approved protocols. Control skin fibroblasts were procured from American Type Culture Collection (Manassas, VA) or Coriell (GM08398, Camden, NJ). Patient and control fibroblasts were grown in high-glucose DMEM (Life Technologies, Carlsbad, CA) supplemented with 10% fetal bovine serum and 1% Antibiotic-Antimycotic (Life Technologies, Carlsbad, CA). Cultured fibroblasts were incubated in a humidy controlled environment at 37°C, with 95% O_2 and 5% CO_2, fed fresh media every 3 days, and were used before passage 10.

Total RNA was isolated from each cell line according to the instructions of the RNeasy Mini Kit (Qiagen, Valencia, CA). Purified RNA was reverse transcribed using First-strand cDNA Synthesis (Origene, Rockville, MD). Real-time quantitative PCR was carried out on the ABI PRISM 7000 Sequence Detection System using TaqMan Universal PCR Master Mix and

TaqMan Gene Expression Assays for human *MED23* (Hs00606608_m1), for human *FOS* (Hs04194186_s1), for human *JUN* (Hs01103582_s1), and *GAPDH* (Hs02758991_g1) (Life Technologies, Grand Island, NY). Expression levels of each transcript were normalized to *GAPDH*.

Allele frequencies were quantified using the RainDrop Digital PCR System (RainDance Technologies, Inc., Billerica, MA). Custom TaqMan SNP Genotyping Assays were designed for both mutations (LifeTechnologies, Grand Island, NY). Digital PCR was performed on patient and control cDNA according to the manufacturer's instructions. Briefly, the 40 uL reaction mixture (50 ng cDNA, 1X TaqMan SNP Genotyping Assay, 1X TaqMan Genotyping Master Mix, and 1X Droplet Stabilizer) was emulsified into uniform droplets using the RainDrop Source machine. PCR amplification was then performed in a BioRad MyCycler thermal cycler (BioRad Laboratories, Hercules, CA) using a 0.5°C per second ramp speed and the following cycling parameters: 10 minutes at 95°C, then 40 cycles of 95°C for 15 seconds and 60°C for 1 minute, followed by an additional 10 minutes at 95°C. The resulting fluorescence of three million droplets per reaction was measured on the RainDrop Sense machine and allele frequencies were calculated using RainDance Analyst software (RainDance Technologies, Inc., Billerica, MA).

Western Blot Analysis

Nuclear proteins were isolated from patient and control skin fibroblasts according to the instructions of the Qproteome Cell Compartment Kit (Qiagen, Valencia, CA). Proteins were then resolved by SDS-PAGE and transferred to a nitrocellulose membrane. The blot was incubated with antibodies against MED23 (BD Pharmingen, San Jose, CA) and histone H2B (EMD Millipore, Billerica, MA) and visualized using the Odyssey CLx infrared imaging system (LI-COR Biosciences, Lincoln, NE).

CLINICAL PRESENTATION

Patient 1

Patient 1 was an 11 year-old Caucasian male who presented to the Undiagnosed Diseases Program (UDP) at the National Institutes of Health (NIH) with profound developmental delay, spasticity, and static encephalopathy. He was the eldest of four brothers in a non-consanguineous family of maternal Hungarian and paternal Czechoslovakian and Polish ethnicity. Notable features, such as birth measurements and abnormal behavioral findings from infancy are described in Table I. He had a small ventricular septal defect (VSD) and patent foramen ovale that closed spontaneously.

From early infancy, he exhibited globally delayed development without regression. He rolled over at age 2 years, sat by age 3 years, scooted at age 5 years, and walked with the assistance of a walker and ankle foot orthoses by age 6 years. On the Vineland Adaptive Behavioral Scales [Sparrow et al., 2005] at age 11 years, he scored below the first percentile for chronological age in communication, daily living skills, socialization, and adaptive behavior composite. Concurrent testing with the Mullen Scales of Early Learning [Mullen, 1995]

placed him at the age-equivalent of 14 months for visual reception, 8 months for fine motor, 10 months for receptive language and 4 months for expressive language.

Muscle spasticity and abnormal movements began in infancy and led to a clinical diagnosis of cerebral palsy by age 1 year. Remarkable neurologic features at age 11 years are described in Table I. His markedly delayed fine motor skills impaired self-feeding, although he demonstrated willingness and ability to learn. After thorough cognitive and motor phenotyping, he was given the diagnosis of profound intellectual disability with co-morbid motor impairments [APA, 2013].

Abnormal brain imaging and EEG studies at age 11 years are summarized in Table I and Figure 1. The EEG was indicative of mild cerebral dysfunction and predisposition to partial or generalized seizures due to unprovoked and photic-provoked epileptiform abnormalities.

Patient 2

Patient 2 was the five year-old brother of patient 1. He presented to the UDP at 22 months with profound developmental delay, spasticity, and poor visual behavior. Birth information and behavioral findings from infancy are listed in Table I. He had a moderate secundum atrial septal defect (ASD) with right ventricular dilation and volume overload which resolved spontaneously. Eye examinations in the first year of life showed brief fixation, inability to track in any direction, and intermittent right exotropia.

Similar to his older brother, patient 2 had global developmental delay that was exacerbated by visual cortical impairment. On the Vineland Adaptive Behavior Scales [Sparrow et al., 2005], he scored below the first percentile in communication, daily living skills, socialization, and adaptive behavior composite at age 5 years. On the Mullens Scales of Early Learning [Mullen, 1995], he obtained an age-equivalent of 3 months for visual reception, 2 months for fine motor, 4 months for receptive language, and 7 months for expressive language.

He also had muscle spasticity and abnormal movements leading to a clinical diagnosis of cerebral palsy by age 1 year. Significant neurologic findings are listed in Table I. At 22 months, he maintained a predominantly flexor position, but could lift his head and shoulders when prone, pull himself forward slightly using his elbows and roll to each side. By age 5 years, he maintained a sitting position with minimal support. After thorough phenotyping, he was diagnosed with profound intellectual disability with co-morbid motor and visual impairments [APA, 2013]

Imaging and EEG anomalies at age 5 years are summarized in Table I and Figure 1. His EEG indicated moderate-to-severe cerebral dysfunction with a disorganized slow background and predisposition to partial or generalized seizures due to bilateral frontal predominant epileptiform abnormalities.

RESULTS

To identify putative genomic causes for their disease, the propositi underwent array CGH and WES. The array CGH did not identify any pathological deletions or duplications. WES

identified variants in 12 genes segregating with disease and meeting frequency and predicted deleteriousness requirements (Supplementary Table 2). Ten mutations did not validate by Sanger sequencing (Supplementary Table 1) leaving the compound heterozygous mutations for *CFCTL* and *MED23.* We considered the mutations in *CFCTL* an unlikely cause of disease because it had no known disease association, and because one mutation was intronic and the other was a polymorphism (frequency: 1–3%, rs146560816). In contrast, *MED23* had been associated with disease and had compound heterozygous mutations (NM_015979.3: c. [3656A>G];[4006C>T]) predicted to encode a deleterious missense mutation (NP_057063.2: p.[H1219R],) and a premature stop codon (p.[R1336X]) (Fig. 2).

The father was heterozygous for c.4006C>T (p.R1336X), and the mother was heterozygous for c.3656A>G (p.H1219R). Real-time quantitative PCR of RNA isolated from patient and control skin fibroblasts detected no marked reduction in steady state levels of (mRNA)*MED23* (Fig. 2). Allele-specific digital PCR confirmed a 1:1 ratio of steady state mRNA from the two mutant *MED23* alleles (data not shown), further excluding nonsense-mediated mRNA decay. Immunoblot analyses of nuclear lysates revealed no alteration in MED23 steady state protein levels (Fig. 2); the resolution of the immunoblot was insufficient to detect whether a stable truncated MED23 protein (150 kDa versus 147 kDa) was produced from the c.4006C>T (p.R1336X) allele.

Confirming the functional significance of the identified mutations, cultured skin fibroblasts from Patient 1 had a similar alteration of the immediate early gene response to serum mitogens as the cultured fibroblasts of the previously reported patients [Hashimoto et al., 2011]. Using qRT-PCR, we observed down regulation of *JUN* expression and up regulation of *FOS* expression (Fig. 2E and F).

DISCUSSION

We report the first non-consanguineous family in which ID cosegregated with compound heterozygous mutations in *MED23*. The mutations (p.H1219R and p.R1336X) did not alter steady-state protein levels in cultured skin fibroblasts suggesting that both mutant proteins are incorporated into the Mediator complex. Similarly, the homozygous p.R617Q MED23 mutation, reported in five affected individuals of a consanguineous Algerian family, did not alter the stability of MED23 or the Mediator complex.

Although the propositi overlap phenotypically with the previously reported cases, there are some important differences. The two Algerian probands, age thirty-nine and forty-one, had mild-to-moderate ID affecting only their ability to read, write, and look after their financial affairs; they had no pathological physical, brain imaging, or EEG findings [Hashimoto et al., 2011]. In contrast, our patients were completely dependent for all activities of daily living and had spasticity, cardiac anomalies, brain malformations, abnormal EEGs and visual impairment (patient 2).

In addition to neurodevelopment, MED23 has a role in cardiovascular development. In zebrafish, *Med23* knockdown causes shortened body length, a ventrally curved tail, heart edema, and bradycardia [Yin et al., 2012]. Knockout of (MOUSE)*Med23* was embryonic

lethal between E 9.5 and 10.5 due to systemic circulatory failure [Balamotis et al., 2009]. Other subunits of the Mediator complex have also been shown to affect cardiovascular development in murine model systems. (MOUSE)*Med1* null embryos develop cardiac malformations, particularly ventricular hypoplasia [Landles et al., 2003], and (MOUSE)*Med12* hypomorphic mutants fail to develop beyond E 10 due to severe defects in neural tube closure, axis elongation, and heart formation [Rocha et al., 2010]. Consequently, the mutations in (HUMAN)*MED23* might explain the congenital heart defects of the propositi.

In summary, the propositi expand the phenotype observed with mutations in *MED23* to include severe ID and spasticity, cardiac anomalies, brain malformations and visual impairment (patient 2 only). In addition, these patients illustrate the power of exome sequencing to identify the genetic basis of disorders without established pathognomonic features.

Supplementary Material

Refer to Web version on PubMed Central for supplementary material.

Acknowledgments

The authors wish to thank the patients, their family and the treating physicians for their cooperation, encouragement and interest in the development of this manuscript. The authors have no conflicts of interest to declare.

References

American Psychiatric Association (APA). Diagnostic and statistical manual of mental disorders. 5. Arlington, VA: American Psychiatric Publishing; 2013.

Balamotis M, Pennella M, Stevens J, Wasylyk B, Belmont A, Berk A. Complexity in Transcription Control at the Activation Domain-Mediator Interface. Sci Signal. 2009; 2(69):ra20. [PubMed: 19417216]

Hall, J., Froster-Iskenius, U., Allanson, J. Handbook of normal physical measurements. Oxford: Oxford University Press; 1989. p. 84

Hashimoto S, Boissel S, Zarhrate M, Rio M, Munnich A, Egly J, Colleaux L. MED23 mutation links intellectual disability to dysregulation of immediate early gene expression. Science. 2011; 333(6046):1161–1163. [PubMed: 21868677]

Kaufman L, Ayub M, Vincent J. The genetic basis of non-syndromic intellectual disability: a review. J Neurodev Disord. 2010; 2(4):182–209. [PubMed: 21124998]

Kaufmann R, Straussberg R, Mandel H, Fattal-Valevski A, Ben-Zeev B, Naamati A, Shaag A, Zenvirt S, Konen O, Mimouni-Bloch A, Dobyns W, Edvardson S, Pines O, Elpeleg O. Infantile cerebral and cerebellar atrophy is associated with a mutation in the MED17 subunit of the transcription preinitiation Mediator complex. Am J Hum Genet. 2010; 87(5):667–670. [PubMed: 20950787]

Kuczmarski, RJ., Ogden, CL., Guo, SS. Vital Health Stat. Vol. 11. Maryland: Department of Health and Human Services; 2002. 2000 CDC growth charts for the United States: Methods and development. National Center for Health Statistics; p. 19-21.

Landles C, Chalk S, Steel J, Rosewell I, Spencer-Dene B, Lalani el-N, Parker M. The thyroid hormone receptor-associated protein TRAP220 is required at distinct embryonic stages in placental, cardiac, and hepatic development. Mol Endocrinol. 2003; 17(12):2418–2435. [PubMed: 14500757]

Leal A, Huehne K, Bauer F, Sticht H, Berger P, Suter U, Morera B, Del Valle G, Lupski J, Ekici A, Pasutto F, Endele S, Barrantes R, Berghoff C, Berghoff M, Neundorfer B, Heuss D, Dorn T, Young P, Santolin L, Uhlmann T, Meisterernst M, Sereda M, Stassart R, Meyer zu Horste G, Nave K, Reis

A, Rautenstrauss B. Identification of the variant Ala335Val of MED25 as responsible for CMT2B2: molecular data, functional studies of the SH3 recognition motif and correlation between wild-type MED25 and PMP22 RNA levels in CMT1A animal models. Neurogenetics. 2009; 10(4):275–287. [PubMed: 19290556]

Markello T, Han T, Carlson-Donohoe H, Ahaghotu C, Harper U, Jones M, Chandrasekharappa S, Anikster Y, Adams D, Gahl W, Boerkoel C. Recombination mapping using Boolean logic and high-density SNP genotyping for exome sequence filtering. Molecular Genetics and Metabolism. 2012; 105(3):382–389. [PubMed: 22264778]

Mullen, E. Mullen Scales of Early Learning: AGS Edition. San Antonio, TX: Pearson; 1995.

NISC Comparative Sequencing Program. NIH Intramural Sequencing Center; Rockville, MD: 2014. http://www.nisc.nih.gov/about.htm

Risheg H, Graham J, Clark R, Rogers R, Opitz J, Moeschler J, Peiffer A, May M, Joseph S, Jones J, Stevenson R, Schwartz C, Friez M. A recurrent mutation in MED12 leading to R961W causes Opitz-Kaveggia syndrome. Nat Genet. 2007; 39(4):451–453. [PubMed: 17334363]

Rocha P, Scholze M, Bleiss W, Schrewe H. Med12 is essential for early mouse development and for canonical Wnt and Wnt/PCP signaling. Development. 2010; 137(16):2723–2731. [PubMed: 20630950]

Schwartz C, Tarpey P, Lubs H, Verloes A, May M, Risheg H, Friez M, Futreal P, Edkins S, Teague J, Briault S, Skinner C, Bauer-Carlin A, Simensen R, Joseph S, Jones J, Gecz J, Stratton M, Raymond F, Stevenson R. The original Lujan syndrome family has a novel missense mutation (p.N1007S) in the MED12 gene. J Med Genet. 2007; 44(7):472–477. [PubMed: 17369503]

Sparrow, SS., Cicchetti, DV., Balla, DA. Vineland Adaptive Behavior Scales. 2. Minneapolis, MN: Pearson Inc; 2005.

Van Bokhoven H. Genetic and Epigenetic Networks in Intellectual Disabilities. Annu Rev Genet. 2011; 45:81–104. [PubMed: 21910631]

Yin J, Liang Y, Park J, Chen D, Yao X, Xiao Q, Liu Z, Jiang B, Fu Y, Bao M, Huang Y, Liu Y, Yan J, Zhu M, Yang Z, Gao P, Tian B, Li D, Wang G. Mediator MED23 plays opposing roles in directing smooth muscle cell and adipocyte differentiation. Genes Dev. 2012; 26(19):2192–2205. [PubMed: 22972934]

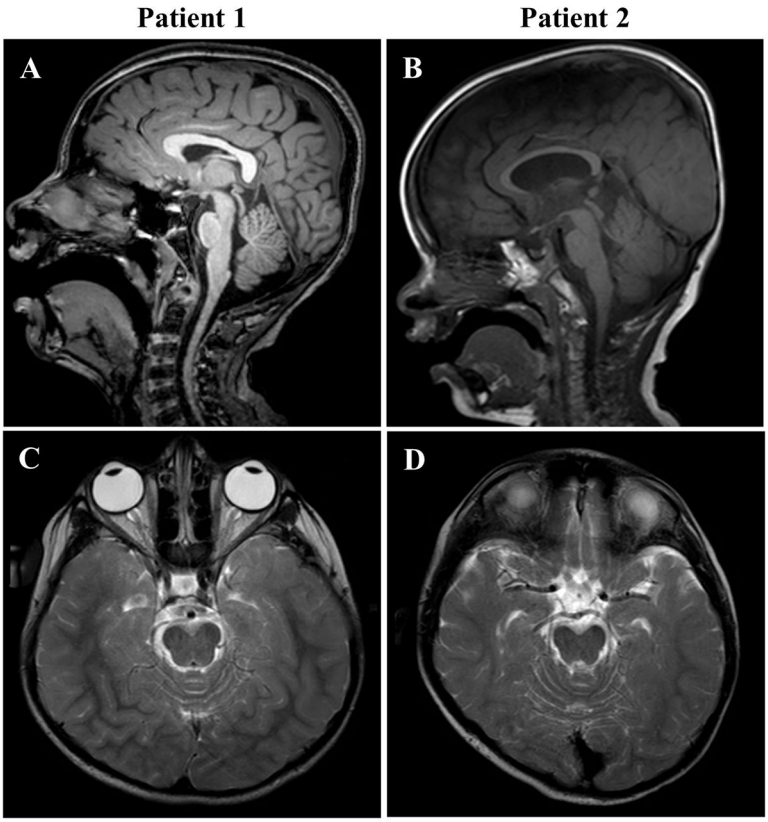

Figure 1.

Mid-line sagittal T1-TFE (Turbo Field Echo) of patient 1 (age 11 years) and T1 of patient 2 (age 22 months) are shown in A and B respectively. Mild-to-moderate pontine hypoplasia was evident in both patients, though less severe in patient 2. Additionally, patient 2 showed mild thinning of the corpus callosum. Axial T2-weighted images of patient 1 (age 8 years) and patient 2 (age 5 years) are shown in C and D respectively. Hypomyelination, as evidenced by reduced gray/white matter differentiation in T2 signal intensity, was noted over the posterior and temporal white matter for both patients. This abnormality resolved by age 11 years in patient 1 (not shown).

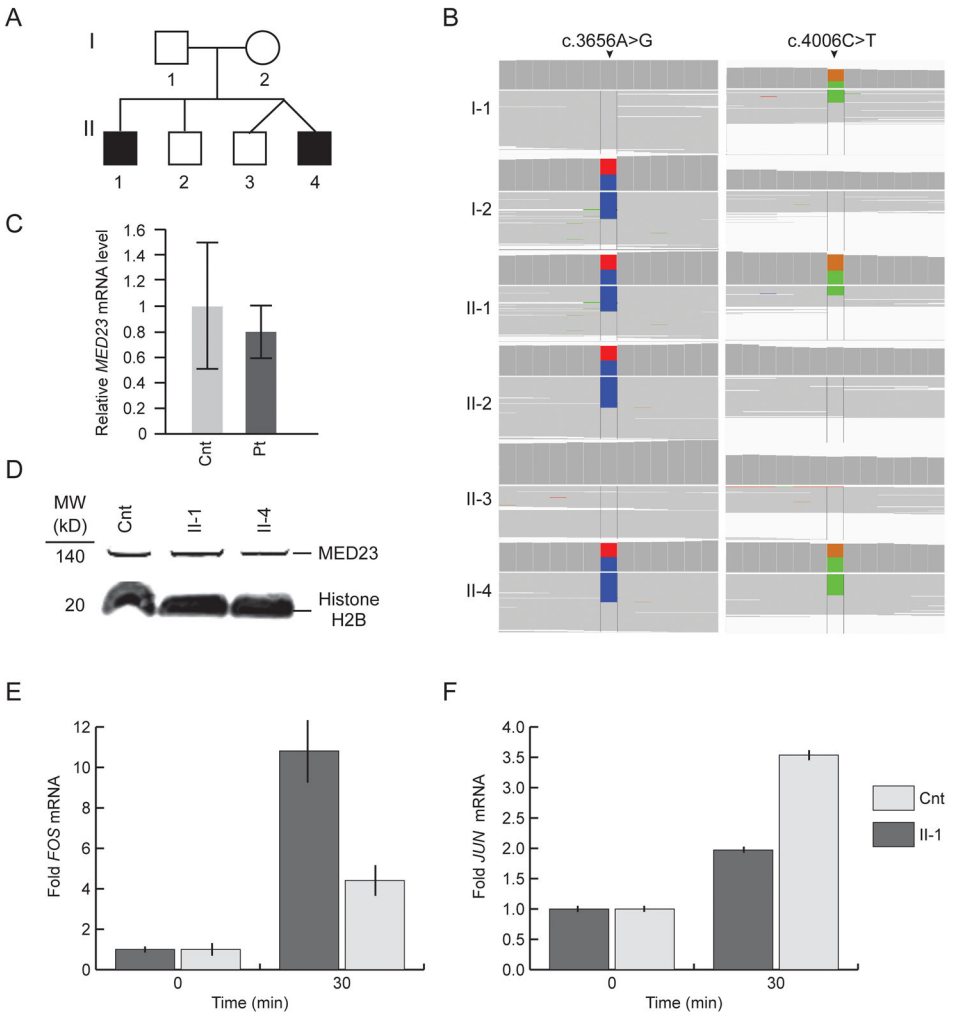

Figure 2.

A) Pedigree of the non-consanguineous family. Squares are males, and the circle is female. The black symbols represent the two affected siblings who presented with profound intellectual disability. B) Whole exome short-read alignments to a human reference genome (hg19) reveal novel *MED23* mutations segregating with disease. The mother was heterozygous for a c.3656A>G (p.H1219R) change (highlighted in blue). The father was heterozygous for a c.4006C>T (p.R1336X) change (highlighted in green). Both affected siblings were compound heterozygous for the mutations. C) Graph showing steady state (mRNA)*MED23* levels detected by qRT-PCR in unaffected control (Cnt) and in pooled patient (Pt) fibroblasts after normalization to *GAPDH.* Error bars represent the standard deviation of four independent experiments. D) Immunoblot detection of MED23 in nuclear lysates from unaffected control (Cnt) and patient fibroblasts. Histone H2B was used as a loading control. E) Plots showing the relative levels of (mRNA)*FOS* in cultured skin fibroblasts of Patient II-1 and an age and gender matched control (cnt). Measurements were made following 24 hours of serum starvation (time = 0) and 30 minutes after addition of serum to 10%. The mRNA levels of three independent replicates were standardized to *GAPDH* mRNA. Error bars represent one standard deviation. F) Plots showing the relative

levels of (mRNA)*JUN* in cultured skin fibroblasts of Patient II-1 and an age and gender matched control (cnt). Measurements were made following 24 hours of serum starvation (time = 0) and 30 minutes after addition of serum to 10%. The mRNA levels of three independent replicates were standardized to *GAPDH* mRNA. Error bars represent one standard deviation.

Table I

Clinical features associated with *MED23* mutations in our patients and those previously reported

Feature	Patient 1	Patient 2	Hashimoto et al. [2011]
Birth Data			
Gestation	40 weeks	36 6/7 weeks (twin)	NR
BW (Weight-for-age Percentile) *	3 kg (50%)	2 kg (5%)	NR
BL (Length-for-age Percentile) *	55 cm (95%)	50 cm (50%)	NR
OFC (Head Circumference-for-age Percentile) **	36 cm (50%)	33 cm (10%)	NR
Apgar Scores	8/9	5/4	NR
Behavioral Findings			
Infant irritability	+	+	NR
Difficulty feeding in infancy	+	+	NR
Sleep dysregulation in infancy	+	+	NR
Childhood screaming spells	+	+	NR
Cardiac			
CHD	VSD	ASD	NR
Current Growth Measurements			
Height-for-age Percentile *	3–10%	25–50%	normal
Weight-for-age Percentile *	10–25%	25–50%	normal
OFC (Head Circumference-for-age Percentile) **	54 cm (75%)	49 cm (5%)	normal
Neurological Findings			
Cognitive impairment	profound ID	profound ID	mild-to-moderate ID
Degree of assistance in ADL	total	total	limited
Static encephalopathy	+	+	NR
Expressive language	−	−	+
Spasticity	+	+	NR
Axial hypotonia	+	+	NR
Dystonia	+	−	NR
Choreoathetoid movements	−	+	NR
Abnormal electroencephalography	+	+	−
Brain Imaging			
Pontine hypoplasia	+	+	−
Thin corpus callosum	−	+	−
Temporal lobe hypomyelination	−	+	−

NR, not reported; VSD, Ventricular Septal Defect; ASD, Atrial Septal Defect; ADL, Activities of Daily Living

* Length and Weight-for-age percentiles were calculated using individual growth charts provided by the Centers for Disease Control and Prevention [Kuczmarski et al., 2002]

** Current Head Circumference-for-age percentiles were calculated using the Handbook of Normal Physical Measurements [Hall et al., 1989]